ACADEMIA ROMÂNĂ
Revue Roumaine de Chimie
https://www.icf.ro/rrch/

Rev. Roum. Chim.,
2025, *70*(1–2), 83–91
DOI: 10.33224/rrch.2025.70.1-2.08

COMPARISON BETWEEN ANALYTICAL SOLUTION OF ADVECTION DIFFUSION EQUATION AND GAUSSIAN PLUME MODEL IN THREE DIMENSIONS THROUGH DIFFERENT STABILITIES

Khaled S. M. ESSA and Hanaa M. TAHA*

Department of Mathematics and Theoretical Physics, Nuclear Research Centre, Egyptian Atomic Energy Authority, Cairo, Egypt

Received October 23, 2024

In this research, the concentration of contaminants was obtained by solving the three-dimensional advection-diffusion equation using the separation of variables technique. Different shapes were adopted for the eddy diffusivity and the logarithmic wind speed under all stability conditions. The analytical results of the advection-diffusion equation were calculated through different stabilities. The calculated results for neutral and stable conditions were compared with already existing observed data for Iodine-131 at the Egyptian Atomic Energy, Nuclear Research Center. Also, the calculated results for unstable conditions were compared with already existing observed data for Iodine-135. Comparisons of the analytical results of the advection-diffusion equation, previous work and the Gaussian plume model, in all stability conditions, are included. Using the statistical methodology, it was discovered that there a strong correlation with the observed concentrations in both neutral and unstable settings compared to stable conditions.

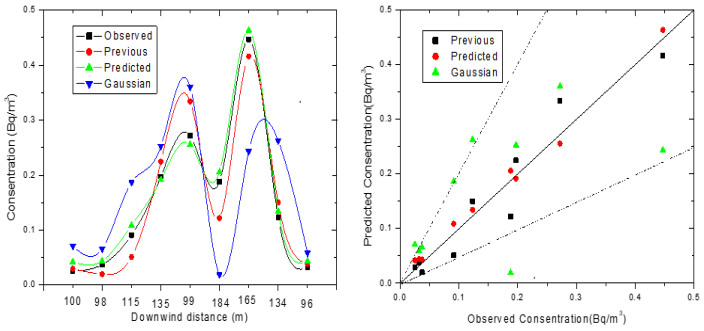

INTRODUCTION

By taking mean wind speed in the neutral case and the eddy diffusivities of pollutants, the advection-diffusion equation was solved in three dimensions space x, y and z using the separation of variables technique to evaluate pollutant concentration per emission rate.[1–7] For the atmospheric dispersion problem, John[8] proposed analytical and approximate solutions under a variety of simplifying assumptions at boundary conditions. Engineers and environmental scientists who researched the transportation of contaminants found particular use in these analytical solutions. A straightforward model for analyzing the dispersion of materials discharged in steady-state releases with brief durations was presented,[9] assuming the existence of an infinite mixing layer. A straightforward method[10] was developed to define surface layer characteristics that characterize vertical diffusion. Hankel transform[11] was used to approximate the solution of the two-dimensional advection-diffusion equation with variable vertical eddy diffusivity and wind speed. Moreover, Hankel transform also was used to get the solution of the three-dimensional advection-diffusion equation.[12]

* Corresponding authors: hanaataha3@yahoo.com; https://orcid.org/0000-0001-7845-1766

The Gaussian plume model[13] was examined as well as the application of the advection-diffusion equation's Gradient Transport (*K*). Atmospheric dispersion models are mostly based on the Gradient Transport (*K*) theory which assumes that the concentration turbulent flux is proportional to the mean concentration gradient, this theory, in addition to other assumptions, gives rise to the advection diffusion equation which was and still widely used in analytical and numerical models of pollution dispersion.

This research estimates the concentration of contaminants under three stabilities situations using various logarithmic wind speed and eddy diffusivity shapes. An analysis of the Gaussian plume model and the analytical version of the advection-diffusion equation are evaluated. The observed isotope data of I^{135} and I^{131} from the Egyptian Atomic Energy Authority are presented. Data on statistical relationships between suggested models, previous[7] and observed concentrations are computed.

MATHEMATICAL TREATMENT

1. Analytical model

In three dimensions, the diffusion equation is

$$u\frac{\partial C(x,y,z)}{\partial x} = \frac{\partial}{\partial y}\left(k_y \frac{\partial C(x,y,z)}{\partial y}\right) + \frac{\partial}{\partial z}\left(k_z \frac{\partial C(x,y,z)}{\partial z}\right) \quad (1)$$

where k_y and k_z are the eddy diffusivities in the vertical and crosswind directions, respectively; *u* is the wind speed (m/s); and *x* is the downwind distance (m). *C*(*x*,*y*,*z*) represents the concentration of pollutants (g/m^3) or (Bq/m^3). The two-dimensional diffusion equation can be obtained by taking crosswind integration with respect to y from –∞ to ∞.

$$u\frac{\partial C_y(x,z)}{\partial x} = \frac{\partial}{\partial z}\left(k_z \frac{\partial C_y(x,z)}{\partial z}\right) \quad (2)$$

where $C_y(x,z)$ is the integrated crosswind pollution concentration. With the following boundary conditions, Eq. (2) is solved:

a) On the ground surface and at the mixing height, the null flux condition is applied.

$$k_z \frac{\partial C_y}{\partial z} = 0 \quad \text{at} \quad z = 0, h \quad (2a)$$

b) When using mass continuity, it is employed.

$$uC_y(0,z) = Q\delta(z - h_s), \ \text{at}\ x = 0 \quad (2b)$$

where δ is a Dirac delta function, hs is a stack height (m), *Q* is the emission rate (g/s) or (Bq/s), and *h* is the height of the atmospheric boundary layer (ABL) (m).

c) When *z* approaches ∞, the crosswind integrated concentration tends to zero.

$$C_y(x,z) \to 0 \quad \text{as } z \to \infty \quad (2c)$$

d) At the mixing height, the crosswind integrated concentration disappears.

$$C_y(x,z) = 0 \quad \text{at } z = h \quad (2d)$$

Taking into account that the height of ABL (*h*) is discretized into *N* sub-interval layers, k_z and *u* are considered as average values within each interval. Subsequently, the solution to Eq. (2) reduces to the solutions of *N* equations of the subsequent kind.

$$u_n(z)\frac{\partial C_y(x,z)}{\partial x} = k_n(z)\frac{\partial^2 C_y(x,z)}{\partial z^2} \quad (3)$$

where

$$k_n(z) = \frac{1}{z_{n+1} - z_n}\int_{z_n}^{z_{n+1}} k_n(z)\ dz$$

$$u_n(z) = \frac{1}{z_{n+1} - z_n}\int_{z_n}^{z_{n+1}} u_n(z)\ dz$$

for, $z_n \le z \le z_{n+1}$, n = 1 : N

Assuming the general solution of Eq. (3) takes the form of separation of variables:

$$C_y(x,z) = X(x)Z(z) \quad (4)$$

By dividing on *X*(*x*)*Z*(*z*) and substituting from Eq. (4) in Eq. (3), one can obtain: -

$$\frac{1}{X(x)}\frac{dX(x)}{dx} = \frac{k_n}{u_n Z(z)}\frac{d^2Z(z)}{dz^2} = -\lambda_l^2 \quad (5)$$

where the constant is λ^2 Eq. (5) can be split into the subsequent two equations:

$$\frac{dX(x)}{dx} = -\lambda_l^2 X(x) \quad (5a)$$

$$\frac{d^2Z(z,h_s)}{dz^2} = -\frac{u_n\lambda_l^2}{k_n} Z(z) \quad (5b)$$

The form of the answers to Eqs. (5a) and (5b) is:

$$X(x) = ce^{-\lambda_l^2 x} \quad (6)$$

$$Z(z) = A_1\cos\left(\lambda_l z\sqrt{\frac{u_n}{k_n}}\right) + A_2 \ \sin\left(\lambda_l z\sqrt{\frac{u_n}{k_n}}\right) \quad (7)$$

where $A_1\ and\ A_2$, and *c* are constants. The answer to Eq. (3) can thus be expressed as follows:

$$C_{yn}(x,z) = c\,A_1 \cos\left(\lambda_l z\sqrt{\frac{u_n}{k_n}}\right) \quad + c\,A_2 \quad \sin\left(\lambda_l z\sqrt{\frac{u_n}{k_n}}\right) \tag{8}$$

when Eq. (8) is applied with the condition of Eq. (2a) at $z = 0$ and $z = h$, $A_2 = 0$ and

$$\lambda_l = \frac{l\pi\sqrt{\frac{k_n}{u_n}}}{h}, l = 0,1,2,\ldots$$

Thus, the following is the answer to Eq. (8):

$$C_{yn}(x,z) = \sum_{l=0}^{\infty} B_l e^{-\lambda_l^2 x}\cos\left(\frac{l\pi}{h}z\right) \tag{9}$$

where, $B_l = c\,A_1$, Using the boundary condition Eq. (2b) and Eq. (4), one gets: $B_0 = \frac{2Q}{hu_n}$, $B_l = \frac{2Q}{hu_n}\cos\left(\frac{l\pi}{h}h_s\right)$, $l = 1,2,3,\ldots$
then

$$C_y(x,z) = \frac{2Q}{hu_n}\left[1 + \sum_{i=1}^{\infty} e^{-\frac{(i\pi)^2}{h^2}\left(\frac{k_n x}{u_n}\right)}\cos\left(\frac{i\pi h_s}{h}\right)\cos\left(\frac{i\pi z}{h}\right)\right] \tag{10}$$

and after that, the following three-dimensional concentration:

$$C(x,y,z) = \frac{2Q}{\sqrt{2\pi}\sigma_y hu_n}\left[1 + \sum_{i=1}^{\infty} e^{-\frac{(i\pi)^2}{h^2}\left(\frac{k_n x}{u_n}\right)}\cos\left(\frac{i\pi h_s}{h}\right)\cos\left(\frac{i\pi z}{h}\right)\right] e^{-\frac{y^2}{2\sigma_y^2}} \tag{11}$$

$$C(x,y,z) = \frac{2Q}{\sqrt{2\pi}\sigma_y hu_n}\left[1 + \sum_{i=1}^{\infty} e^{-\frac{(i\pi)^2}{h^2}\left(\frac{k_n x}{u_n}\right)}\cos\left(\frac{i\pi h_s}{h}\right)\cos\left(\frac{i\pi z}{h}\right)\right] e^{-\frac{y^2}{2\sigma_y^2}-\frac{\lambda x}{u}} \tag{12}$$

for the given nuclide, where $e^{-\frac{\lambda x}{u}}$is the radioactive decay.

2. Gaussian model

Taylor's one-particle dispersion theory provides an description of the total dispersion in a steady plume from a continuous source in a homogeneous flow, while the Gaussian formula is applied to the plume's concentration distribution as follows:

$$C(x,y,z) = \frac{Q}{2\pi\bar{u}\sigma_y\sigma_z} exp\left[-\frac{y^2}{2\sigma_y^2} - \frac{(z-H)^2}{2\sigma_z^2} - \frac{(z+H)^2}{2\sigma_z^2}\right] \tag{13}$$

where the three-dimensional concentration is denoted by $C(x,y,z)$. The average wind speed (m/s) is represented by the variables x, y, z, and $\bar{u}$. The standard deviations in lateral and vertical heights are σ_y and σ_z, where $\sigma = (2kx/u)^{1/2}$and h is the effective height (m) equal to $h_s + 3\left(\frac{w}{u}\right)D$ is the stack diameter, h_s is the stack height, and w is the existing plume velocity. Additionally, the following is the Gaussian plume model through the centerline:

$$C(x,0,z) = \frac{Q}{2\pi\bar{u}\sigma_y\sigma_z}\exp\left[-\frac{(z-H)^2}{2\sigma_z^2} - \frac{(z+H)^2}{2\sigma_z^2}\right]e^{-\frac{\lambda x}{u}} \tag{14}$$

such that, using various stabilities, the values of u_n and k_n are given as follows:

Neutral case

Using $k_n = 0.4\,u_*\,z$ and $u_n = \frac{u_*}{0.4}\,Ln\left(\frac{z+z_0}{z_0}\right)$, in the neutral case,[15] the meteorology under stable and neutral conditions is obtained from Table 1 as follows:

Table 1

The meteorology under stable and neutral conditions during the experiments[14]

Exp	Atmospheric stability	L	u_* (m/s)	u_{27} (m/s)	mixing height (h) (m)
1	D	∞	0.67	5.80	2680
5	E	55	0.50	3.80	209

Table 2 provides the values for the crosswind and vertical standard deviations through stabilities

Table 2

Formulas for $\sigma_y(x)$ and $\sigma_z(x)$ for urban conditions[15]

Stability classes	σ_z (m)	σ_y (m)
A	$0.24\cdot(1+0.001x)^{1/2}$	$0.32\cdot(1+0.0004x)^{-1/2}$
B	$0.24\cdot(1+0.001x)^{1/2}$	$0.32\cdot(1+0.0004x)^{-1/2}$
C	$0.20x$	$0.32\cdot(1+0.0004x)^{-1/2}$
D	$0.14\cdot(1+0.0003x)^{-1/2}$	$0.16\cdot(1+0.0004x)^{-1/2}$
E	$0.08\cdot(1+0.00015x)^{-1/2}$	$0.11\cdot(1+0.0004x)^{-1/2}$
F	$0.08\cdot(1+0.00015x)^{-1/2}$	$0.11\cdot(1+0.0004x)^{-1/2}$

The values of the observed, previous, predicted and Gaussian concentrations for Iodine-131 (I^{131}) are displayed with downwind distance in the neutral situation, as follows in Table 3:

Table 3

The values of the observed, previous, predicted and Gaussian concentrations for Iodine-131 (I^{131}) with downwind distance in the neutral situation

Downwind distance (m)	Observed conc. (Bq/m^3)	Previous work conc. (Bq/m^3)	Predicted conc. Eq. (16) (Bq/m^3)	Gaussian conc. Eq. (16) (Bq/m^3)
100	4.1	6.12	6.56272	6.7
110	3.8	5.58	5.70446	5.9
120	3.8	5.12	5.01984	5.1
130	3.7	4.74	4.46331	4.6
140	3.4	4.41	4.00361	4.1
150	3.2	4.12	3.61866	3.8
160	3.1	3.87	3.29244	3.5
170	3	3.65	3.01312	3.1
180	2.9	3.45	2.77174	3.1
190	2.7	3.28	2.56145	2.9
200	2.4	3.12	2.37691	2.6
300	1.4	2.12	1.32045	1.7
400	0.50	1.62	0.87403	0.9

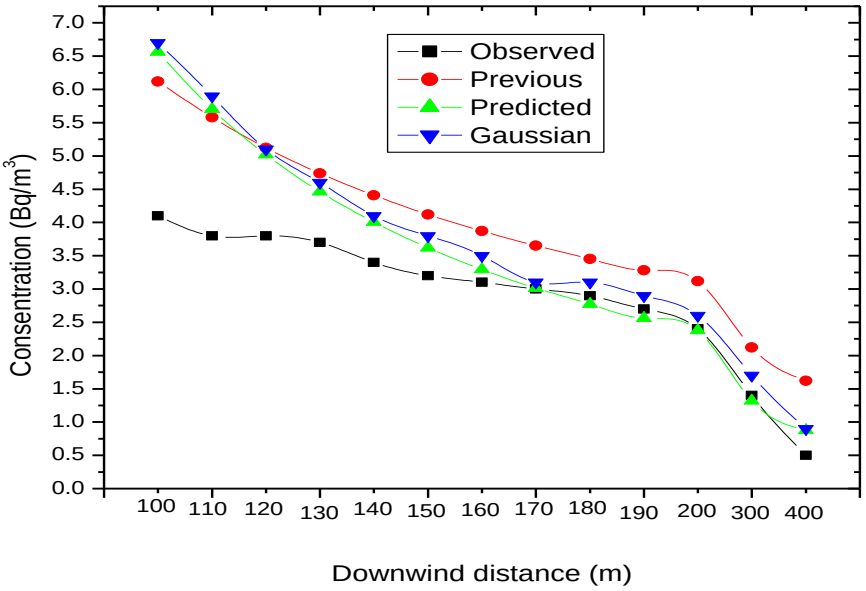

Fig. 1 – demonstrates the change in I^{131} concentrations with downwind distance in the neutral situation.

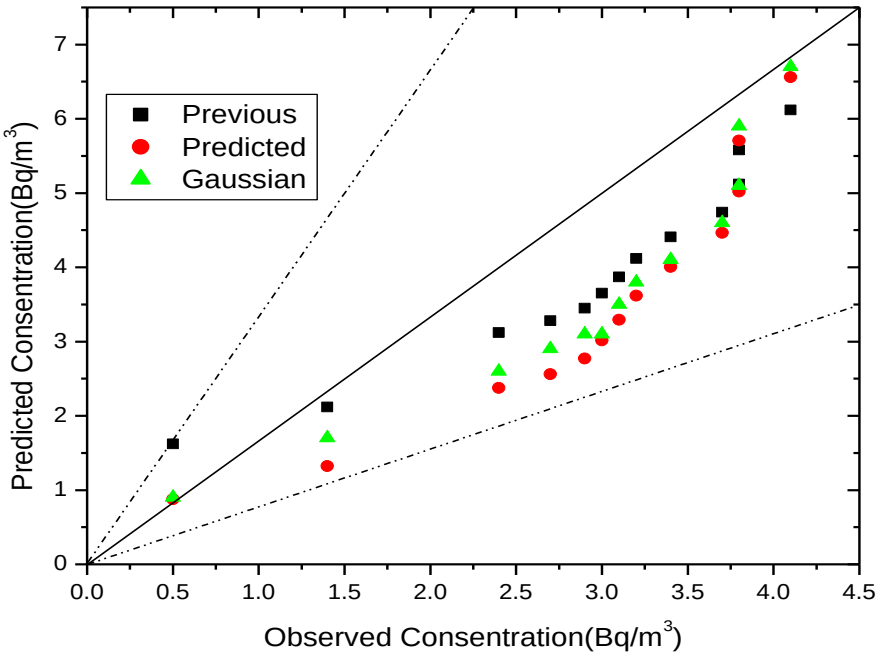

Fig. 2 – displays the I ^{131} observed and projected variability in the neutral condition.

Figure 1 shows that the predicted concentrations of I^{131}as the same as observed concentration with the downwind distance in neutral case. Also, the predicted concentrations are inside a factor of two with the observed concentration data in neutral case as shown as in Fig. 2.

Stable case

Under stable conditions, the wind speed is calculated as[15]

$$u_n = \frac{u_*}{0.4}\left(Ln\ \frac{z+z_0}{z_0} + 5\ \frac{z}{L}\right),$$

and the eddy diffusivity is

$$k_n = 0.4\ u_*\ \frac{z}{1+5\frac{z}{L}}.$$

In the stable situation with downwind distance, the values of the anticipated and observed concentration are displayed as follows in Table 4:

Table 4

The values of the observed, previous, predicted and Gaussian concentrations for Iodine-131 (I^{131}) with downwind distance in the stable situation

Downwind distance (m)	Observed conc. (Bq/m^3)	Previous work conc. (Bq/m^3)	Predicted conc. Eq. (16) (Bq/m^3)	Gaussian conc. Eq. (16) (Bq/m^3)
100	0.25	0.09	0.22868	0.1
110	0.26	0.08	0.199101	0.1
120	0.28	0.07	0.175479	0.09
130	0.28	0.07	0.156255	0.1
140	0.27	0.06	0.14036	0.08
150	0.26	0.06	0.127036	0.08
160	0.25	0.06	0.115735	0.09
170	0.21	0.05	0.10605	0.1
180	0.19	0.05	0.0976732	0.07
190	0.16	0.05	0.0903694	0.06
200	0.11	0.04	0.0839546	0.04
300	0.04	0.03	0.0471094	0.04
400	0.01	0.02	0.0314422	0.02

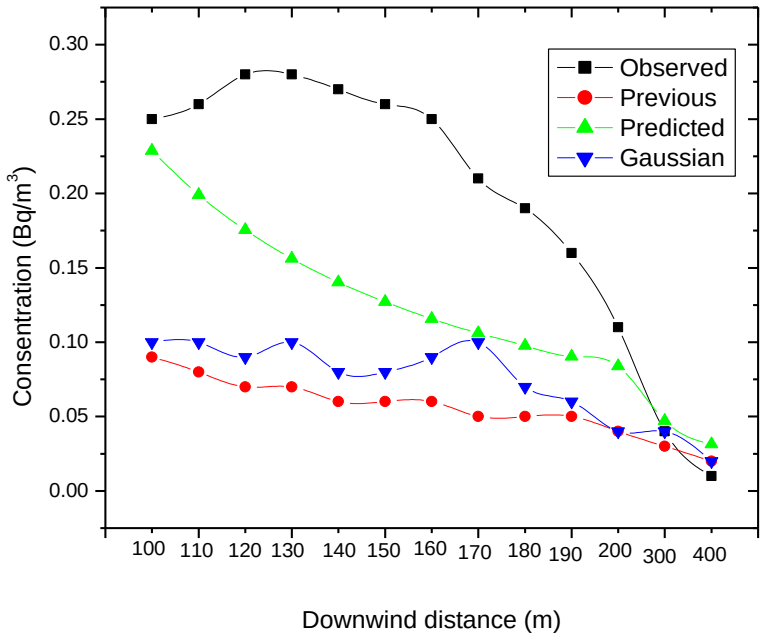

Fig. 3 – displays the change in I^{131} concentrations with downwind distance in the stable scenario.

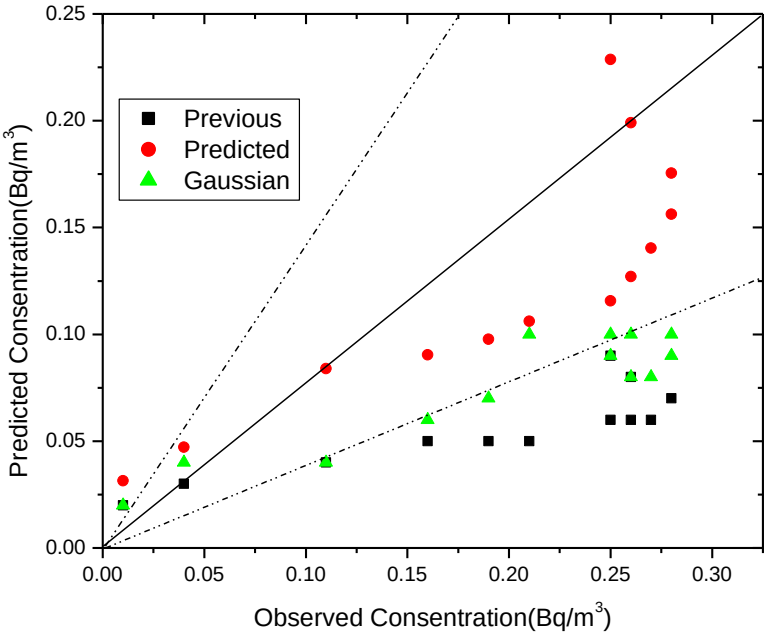

Fig. 4 – Demonstrates the I^{131}expected and actual variability in a stable scenario.

The projected concentrations of I^{131} with the downwind distance in the stable case are smaller than the observed concentrations, as shown in Fig. 3. In the sable scenario, the Gaussian plume model's projected concentrations at most spots match the observed concentration data within a factor of two, which is in line with previous research as illustrated in Fig. 4.

Unstable case

The eddy diffusivity in an unstable case is[15]

$$k_n = 0.4\, u_* \frac{z}{\emptyset\left(\frac{z}{L}\right)},$$ and the wind speed is

$$u_n = \frac{u_*}{0.4}\left(Ln\ \frac{z+z_0}{z_0} - 2Ln\ 0.5\left(1+\frac{1}{\emptyset}\right) - Ln\ 0.5\left(1+\frac{1}{\emptyset^2}\right) + \tan^{-1}\left(\frac{1}{\emptyset}\right) - \frac{\pi}{2}\right),$$

where $\emptyset\left(\frac{z}{L}\right) = \left(1 - 15\ \frac{z}{L}\right)^{-0.25}$ and the following values are assumed: $\lambda = 2.9 \cdot 10^{-5}$; h_s=43 m; z_0 = 0.6 cm; z = 0.7 m and L = –35 m.

Table 5

Weather information from the nine convective test runs conducted in March and May 2006 at the Inshas site, Egypt[16]

Run no.	Working hours of the source	Release rate (Bq)	U10 (m s^{-1})	Wind direction (deg)	U43 (m s^{-1})	W* (ms^{-1})	P-G stability class	*h* (m)	Vertical distance (m)
1	48	1028571	4	301.1	4.97829	2.27	A	600.85	5
2	49	1050000	4	278.7	4.97829	3.05	A	801.13	10
3	1.5	42857.14	6	190.2	7.46744	1.61	B	973	5
4	22	471428.6	4	197.9	5.35493	1.23	C	888	5
5	23	492857.1	4	181.5	4.97829	0.958	A	921	2
6	24	514285.7	4	347.3	5.76006	1.3	D	443	8.0
7	28	1007143	4	330.8	5.35493	1.51	C	1271	7.5
8	48.7	1043571	4	187.6	5.35493	1.64	C	1842	7.5
9	48.25	1033929	4	141.7	4.97829	2.1	A	1642	5.0

Table 6

Meteorological characteristics and concentrations recorded in unstable conditions during the Inshas, Egypt

Run	Stability class	Distance (m)	*Q* (Bq)	Observed *C* (Bq/m^3)	Previous work *C* (Bq/m^3)	Predicted *C* (Bq/m^3)	Gaussian *C* (Bq/m^3)
1	A	100	1028571	0.025	0.0296	0.0418429	0.07065
2	A	98	1050000	0.037	0.0197	0.0436213	0.06579
3	B	115	42857.14	0.091	0.0508	0.108579	0.18675
4	C	135	471428.6	0.197	0.2247	0.191328	0.2527
5	A	99	492857.1	0.272	0.3339	0.255415	0.36027
6	D	184	514285.7	0.188	0.1218	0.205759	0.01877
7	C	165	1007143	0.447	0.4159	0.463389	0.24335
8	C	134	1043571	0.123	0.1500	0.134184	0.26276
9	A	96	1033929	0.032	0.0381	0.0438281	0.05876

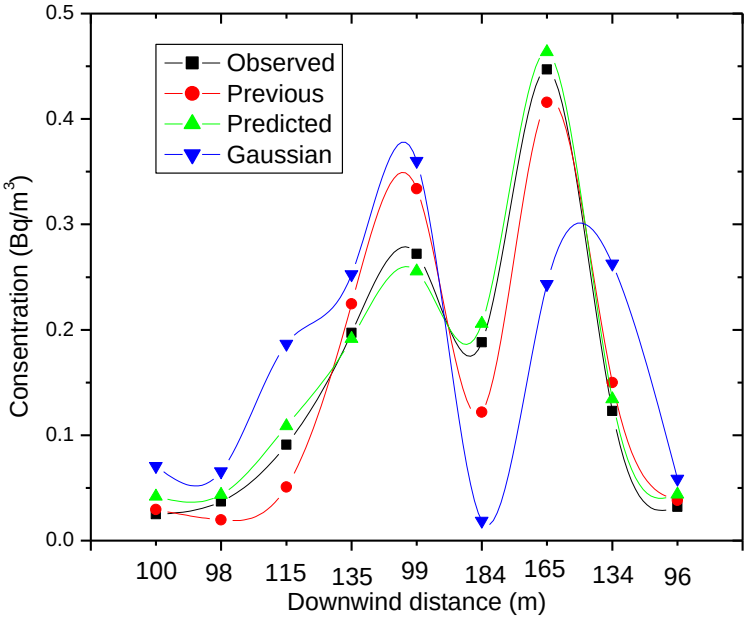

Fig. 5 – Demonstrates how I^{135} concentrations with downwind distance can change in an unstable situation.

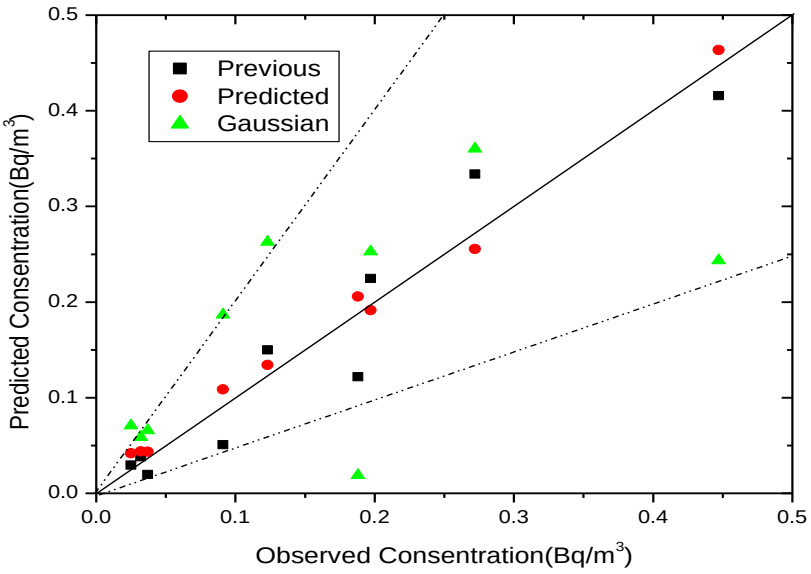

Fig. 6 – Illustrates the I^{135} projected and observed variability in an unstable scenario.

As can be shown in Fig. 5, the concentrations of I^{135} with the downwind distance in the unstable case are identical to those observed in the predicted, Gaussian and prior models. As displayed in Fig. 6 all of the projected concentrations fall within a factor of two with the observed concentration data.

Statistical Methods

Hanna[17] introduced the comparison of observed and projected concentrations.

Table 7

Depicts a comparison of the concentrations in neutral conditions—predicted and observed

	NMSE	FB	COR	FAC2
Predicted	0.09	–0.18	0.92	1.2
Gaussian model	0.10	–0.23	0.92	1.26
Previous model	0.07	–0.29	0.95	1.35

Table 8

Demonstrates a comparison of the concentrations observed and expected under stable conditions

	NMSE	FB	COR	FAC2
Predicted	0.21	0.45	0.83	0.62
Gaussian model	0.96	0.90	0.92	0.38
Previous model	1.6	1.1	0.88	0.28

Table 9

Illustrates how the concentrations in an unstable state compare to the predictions

	NMSE	FB	COR	FAC2
Predicted	0.005	–0.52	1.0	1.1
Gaussian model	0.22	–0.07	0.59	1.1
Previous model	0.05	0.02	0.98	0.96

where FB stands for fraction bias, COR for correlation coefficient, FAC2 for factor of two, and NMSE for normalized mean square error.

Tables (7, 8 and 9) indicate that the statistical methods of the analytical, previous and Gaussian models in both neutral and unstable conditions agree well with the observations than concentration information in a table conditions. Compared to the analytical, Gaussian, and previous models in neutral and unstable conditions, achieved 100%, but in stable conditions, achieved 43%.

CONCLUSIONS

Using the separation variables technique, the three-dimensional Advection-diffusion equation in steady state with continuous point source is solved, taking into account various logarithmic wind speed shapes and eddy diffusivity in all stability conditions. The analytical advection-diffusion equation model was used to calculate the predicted concentrations through different stabilities.

The observed data of radioactive I^{135} in unstable situations and I^{131} in neutral and stable conditions conducted at the Egyptian Atomic Energy Authority[16, 14] were used to compare the outcomes of the suggested three dimensional. Advection diffusion equation model, Gaussian, and prior model. We found that under neutral and unstable conditions, the projected concentration data agree with the observed concentration data far better than under stable conditions. Additionally, statistical evidence indicates that the projected concentrations

agree with the observed values by a factor of two. The anticipated and observed concentrations data agree better under neutral and unstable settings than under stable ones, according to the NMSE, FB, and COR values for the predicted concentrations. Compared to the analytical, Gaussian, and previous models in neutral and unstable conditions, achieved 100%, but in stable conditions, achieved 43%.

REFERENCES

1. J. S. Lin and L. M. Hildemann, *Atmospheric Environ.*, **1996**, *30*, 239–254.
2. K. M. Singh and M. Tanaka, *Eng Anal Bound Elem*, **2000**, *24*, 225–235.
3. P. Kumar, "Analytical Models for Dispersion of Pollutants in the Atmospheric Boundary Layer", *Ph.D*. Thesis, Indian, Institute of Technology Delhi, 2010.
4. K. S. M. Essa and S. E. M. Elsaid, *Pyrex J. Ecology Natural Environ.,* **2015**, *1*, 001–006.
5. K. S. M. Essa, S. E. M. Elsaid and F. Mubarak, *J. Atmosphere*,**2015**, *1*, 8–16.
6. K. S. M. Essa, S. M. Etman and M. El-Otaify, *Rev. Brasileira de Meteorologia*, **2014**, *29*, 125–138.
7. K. S. M. Essa, S. M. Etman, M. S. El-Otaify, *Climate Change*, **2016**, *2*, 180–191.
8. J. M. Stockie, *SIAM Review*, **2011**, *53*, 349–372.
9. E. Palazzi, M. De Faveri, G. Fumarola and G. Ferraiolla, G., *Atmospheric Environ.*, **1982**, *16*, 2785–2790.
10. A. P. Van Ulden, *Atmospheric Environ.,* **1978**, *12*, 2125–2129.
11. K. S. M. Essa, A. S. Shalaby**,** M. A. E. Ibrahim and A. M**.** Mosallem, *Pure Appl. Geophys.*, **2020**, *177*, 4545–4557, DOI: 10.1007/s00024-020-02496-y.
12. K. S. M. Essa, A. M. Mosallem and A. S. Shalaby, *Atmospheric Sci. Lett.*, **2021**, *22*, 1–7, DOI: 10.1002/asl.1043.
13. K. S. M. Essa and H. M. Taha, *MAUSAM*, **2023**, *74*, 663–672.
14. K. S. M. Essa, *Arab J. Nuclear Sci. Appl.*, **2009**, *42*, 123–130.
15. S. R. Hanna, G. A. Briggs and R. P. Jr. Hosker, DOE TIC-11223 (DE 82002045) 1982.
16. IAEA "Atmospheric Dispersion in Nuclear Power Plant Siting", S.S. No. 50-SG-S3, IAEA-Vienna, 1980.
17. S. R. Hanna, *Atom. Environ*. **1989**, *23*, 1385–1395.